Iranian Journal of Hydrogen & Fuel Cell 2(2019) 163-170

Iranian Journal of Hydrogen & Fuel Cell

IJHFC

Journal homepage://ijhfc.irost.ir

Synthesis and Characterization of Co-doped CeO_2 Ceramic Electrolyte for IT-SOFC

Rabia KIRKGEÇİT[1], Handan ÖZLÜ TORUN[2*]

[1]KahramanmaraşSütçü İmam University, Institute of Science, Material Science and Engineering, Kahramanmaraş, 46050, Turkey
[2]KahramanmaraşİstiklalUniversity, Elbistan Engineering Faculty, Department of Energy Systems Engineering, Kahramanmaraş , 46300, Turkey

Article Information

Article History:

Received:
12 Dec 2019
Received in revised form:
1 Feb 2020
Accepted:
4 Feb 2020

Keywords

CeO_2
Intermediate temperature solid oxide fuel cell
Solid electrolyte

Abstract

Solid oxide fuel cells are electrochemical systems. One of the most important compounds in their structure is the ceramic electrolyte. The ceramic electrolyte property of the CeO_2 compound is currently being investigated in many studies. In this study, we tried to synthesize different CeO_2 compounds. $Ce_{0.85-x-y}La_xGd_yO_2$ nanocrystalline powders were prepared via the hydrothermal method. Phases identification was completed through X-ray diffraction, SEM-EDS, thermal and impedance analysis. XRD data showed that all the obtained powders had a cubic fluorite structure. After examining the surface images, it was seen that the particle sizes were on the micron scale. Impedance measurements of the pelletized sample were also made. The $Ce_{0.85-x-y}La_xGd_yO_2$ poweder was sintered at 1250 °C. Increased conductivity value was calculated with increasing temperature. The best conductivity was observed at 750 °C and the conductivity value was 0.0022 $S.cm^{-1}$. The results indicated that the degree of electrical conductivity was found to be low regarding the applications in intermediate temperature solid oxide fuel cells.

1. Introduction

Due to increasing world population, the need for energy is rising. However, due to the rapid depletion of fossil resources in the world, the interest in renewable energy resources is increasing day by day. Renewable energy is the type of energy considered as an alternative to traditional fossil fuels, and

*Corresponding Author's Fax: +90 3443004102
E-mail address: handanozlu@gmail.com

doi: 10.22104/ijhfc.2020.3961.1198

intensive work has been carried out on it in recent years. Renewable energy is a type of continuously produced energy obtained from natural sources, unlike fossil fuels. Scientists thatwork on hydrogen energy in renewable energy sources have reported that it will play a major role in energy production in the future. One of the most striking of the new generation of energy sources is hydrogen energy and it is used in fuel cells [1]. A fuel cell produces electrical energy as a result of a chemical reaction. Advantages of fuel cells include lack of charge/discharge problems, dimensional flexibility, portability, and low pollution levels [2, 3]. Fuel cells can be classified in different ways. The most common way is to divided them into six classes according to the the type of electrolyte used. These are the i) proton exchange membrane fuel cell, ii) alkaline fuel cell, iii) phosphoric acid fuel cell, iv) molten carbonate fuel cell, v) solid oxide fuel cell, and vi) direct methanol fuel cell [4]. Solid oxide fuel cells operate at higher temperatures than other fuel cells and are very efficient. They can be used as a cogeneration unit with waste heat as well as electrical energy. Due to these properties, solid oxide fuel cells can also be used in combination with gas cycles [5-9]. Solid oxide fuel cells are the systems that produce electricity as a result of a chemical reaction between fuels such as hydrogen, methane and oxygen. They consists essentially of a triple structure including an anode (fuel electrode) / ceramic electrolyte / cathode (air electrode). However, high temperature limits the feasibility of solid oxide fuel cells as it increases system costs as operating temperatures above 700 oC restrict the selection of materials suitable for the construction of the stack [10]. The first step in solving this problem is the selection of an electrolyte to be used in the cell. The selected electrolyte must be an oxygen ion conductor, aintain thermal stability at high temperatures, and its oxygen pressure should be good, dense, fine, and mechanically compatible with other components [11]. For this purpose, compounds such as ZrO_2, Bi_2O_3, $LaGaO_3$, and CeO_2 are used in solid oxide fuel cells [4,11-16]. Of these, the compound most commonly used at low temperatures is CeO_2.

Although the CeO_2 compound is not a good oxygen conductor in its pure state, the conductivity properties can be improved by adding different elements. Due to the Krönk-Ving equation, the amount of oxygen space increases and accelerates the oxygen delivery [6]. The selection of ionic radius, impurities amount, doping method, and sintering temperatures are important in conductivity studies. The ion radius of the dope compounds to be selected must be higher than the critical radius value, which improves the conductivity properties. At the same time, the crystal size of the nanostructures and grain formation after sintering positively affects the conductivity. In general, a trivalent doping additive has higher conductivity than a bivalent additive. There is also an optimum cation radius value for the highest ionic conductivity of the trivalent doped CeO_2 (1.024 Å). In the case of triple additions, the ion radii of the compounds to be doped are close to the optimum radius value and this affects the conductivity values [17-24].

In our study, CeO_2 electrolyte was selected for intermediate temperature applications and usage. The contribution of two different types of (+3) value cations on the conductivity was also investigated. Accordingly, dope elements were carried out using the hydrothermal method. The crystalline, thermal, microstructural, and electrical properties of the obtained compounds were investigated in detail.

2. Materials and Methods

The La and Gd doped ceria nanomaterials $Ce_{0.85-x-y}La_xGd_yO_2$ was prepared by using the hydrothermal method. The starting materials were [Ce $(NO_3)_3.6H_2O$] (Sigma-Aldrich 99.99%), [$La(NO_3)_3.6H_2O$] (Sigma-Aldrich 99.99%), and [$Gd(NO_3)_3.6H_2O$] (Sigma-Aldrich 99.99%) powders. Stirring was continued on the magnetic table until the precipitation was completed. A 6 M NaOH solution was used for precipitation. The heterogeneous solution was transferred to a teflon coated stainless steel autoclave (12 hours, 180 °C). After the

hydrothermal treatment, the solution was filtered, washed, and dried at room temperature. Then the dried powders were ground with an agate mortar and heat-treated at 800 °C for 12 hours. Also, the powder sample was made ready for the electrolyte (Fig. 1). The powder samples for conductivity measurements were pressed using a hydraulic press under 10 bar pressure. A 13 mm diameter pellet was obtained. The pressed disk was sintered in air at 1250 °C for 12 hours. The x-ray diffraction technique was used to determinate the crystal structure, lattice parameter, and purity. The XRD used a Philips X 5 Pert Pro(λ = 0.154056 nm, Cu-Kα radiation). After pre-drying, the prepared $C_{e0.85}La_{0.1}Gd_{0.05}O_2$ was blended and the powders were analysed by TG/DTA control. Depending on the increasing temperature, the mass changes of the material were analyzed at a constant heating rate of 1000 °C with an increase of 10 °C / min. In order to determine the morphology and microstructure of the sintered samples, the electrolytes pressed into the disc were analysed using a Zeiss EVO 10LS brand microscope. The ionic conductivity measurements were obtained with an AC impedance analyzer (Parstat 2273) at a temperature range of 400 to 750 °C.

3. Results and Discussion

3.1. XRD Analysis

The XRD pattern of the Ce based La, Gd co-doped samples and pure CeO_2 are shown in Fig. 2. According

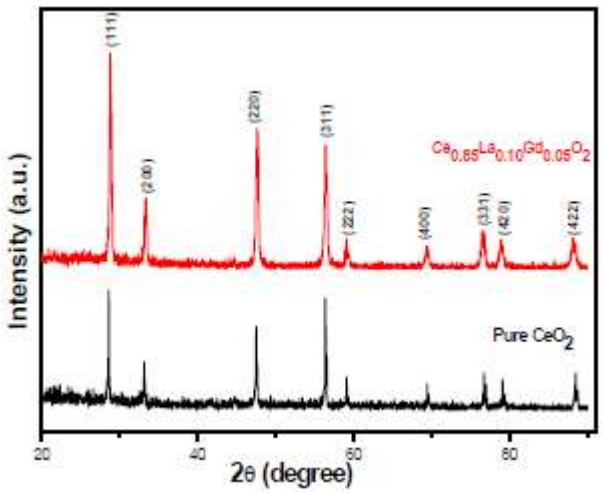

Fig.2 XRD of pure CeO_2 and $Ce_{0.85}La_{0.1}Gd_{0.05}O_2$ powder

to the powder electrolyte with cubic crystal lattice values, which were obtained by hydrothermal synthesis, the patterns are good agreement with the pattern (ICSD 98-015-5618). The x-ray diffraction result obtained after the synthesis process is compatible with the pure CeO_2 structure.

The unit cell parameter of the sample is (Å) = 5.4724. The pure CeO_2 unit cell parameter is 5.411 Å. The unit cell parameter increase is due to the ionic radius values of Gd^{3+} (1.053 Å) and La^{3+}(1.16 Å). The narrow spectral width characteristic peaks indicate that the products are highly crystalline. The crystalline size co-doped CeO_2 were calculated with Debye-Scherrer equations (Eqs. (1)). The sharpest peaks in the plane of (111) (200) (220) (311) were used to calculate the crystal size. As a result of calculations, the crystalline size of $Ce_{0.85}La_{0.1}Gd_{0.05}O_2$ powder is 36.46 nm.

Fig. 1. Flow chart of hydrothermal method

$$D = \frac{0.89\lambda}{\beta \cos\theta} \qquad \beta = \beta_{obs} - \beta_{std} \tag{1}$$

$$\varepsilon = \frac{\beta}{4\tan\theta} \qquad \beta = \sqrt{\left(\beta_{obs}{}^2 - \beta_{std}{}^2\right)} \tag{2}$$

3.2 Thermal Analysis

The properties of material were examine as a function of temperature with the thermal analysis method. It is useful to determine phase changes, dissociate, determine species (such as nitrate, water, and oxygen loss), and generate phase diagrams. The thermal decomposition behaviour of the $Ce_{0.85}La_{0.1}Gd_{0.05}O_2$ powder is shown in Fig. 3. Examining the TG curve in Fig. 3, the loss of mass is seen to be quite low (about 10%) in the sample powder subjected to heat treatment This loss is due to incomplete drying after filtration and species, such as nitrate, found in the structure. After 600 °C, there was almost no loss of mass. The DTA curve gives one endothermic peaks around 100 °C. Above this temperature, the phase remained stable.

3.3. Microstructure and Electrical Conductivity

SEM-EDS was used to examine surface structure and micro defects in the pellet and to detect the ratio of elements. Microstructures of the synthesized powders were examined before pressing and sintering. The surface images of the samples sintered at 800 °C after hydrothermal treatment are given in Fig. 4a. Grain sizes range from 120 to 170 nm. In EDS analysis evaluation, it is seen that the synthesis rates are close to the calculated rate. In the next step, the powder samples were pelleted and sintered at 1250 °C. $Ce_{0.85}La_{0.1}Gd_{0.05}O_2$ condensed at 1250 °C and has electrolyte and uniform grain sizes (~2μ). The particle size increased with the effect of temperature and pressure. As shown in Figure 4b, when the images taken from different points are evaluated, pore formation on the surface is quite low. This situation is due to low sintering temperature (1250 °C). According to the EDS results for all sample, as illustrated in Table 1, the final electrolyte ratios were found to be similar with that of the initial stoichiometric ratios.

Impedance spectroscopy was used for the electrical characterization of the synthesized sample. Impedance spectroscopy is the preferred technique to examine the electrical properties of ceramic electrolytes. Calculation of total ionic conductivity by impedance spectroscopy also provides information

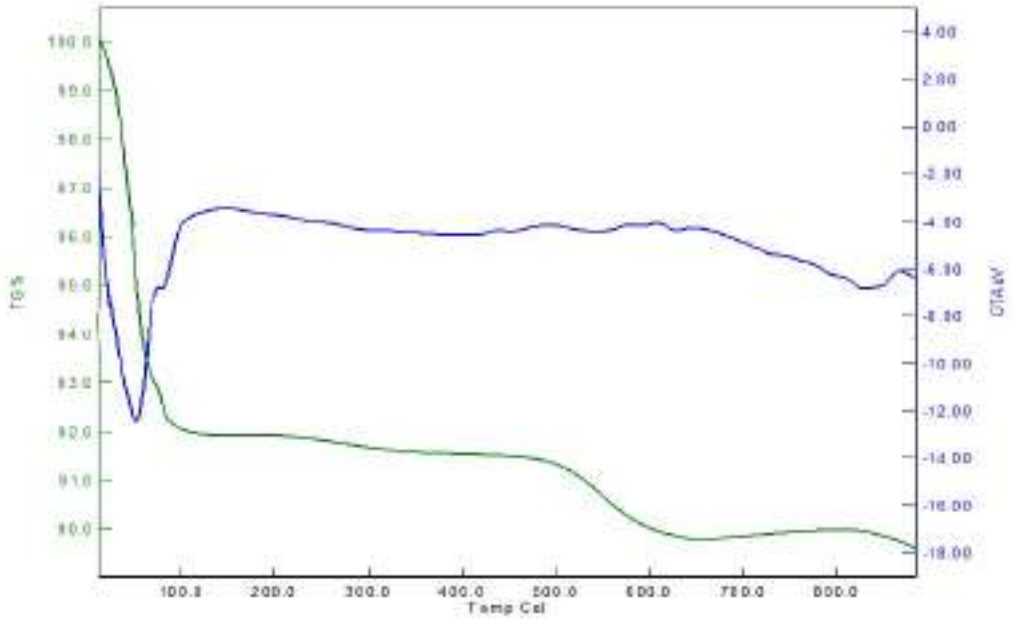

Fig.3. TG/DTA graphics of pre-dry $Ce_{0.85}La_{0.1}Gd_{0.05}O_2$ of powder

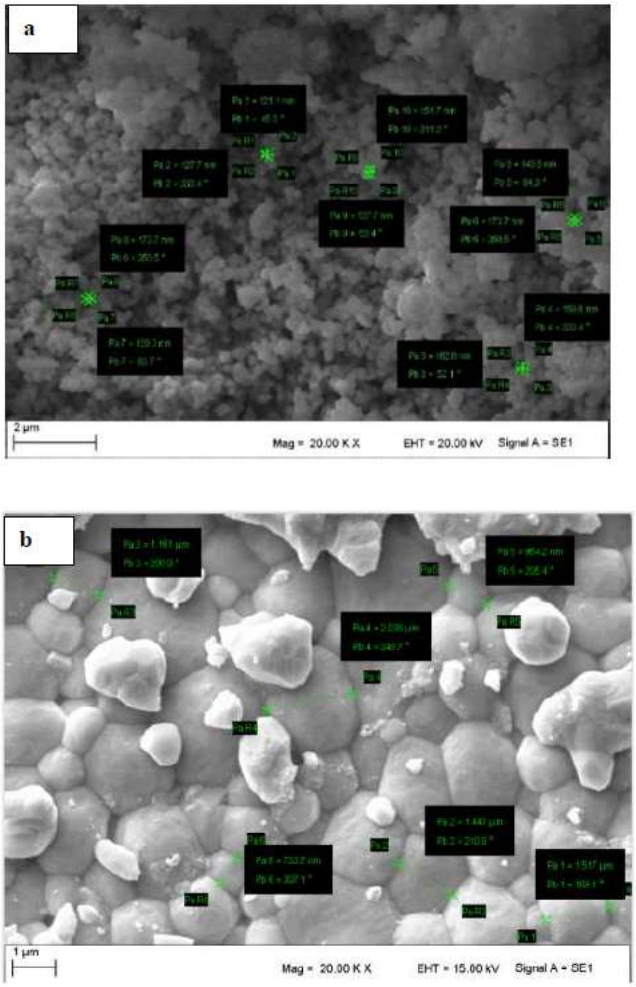

Fig. 4. Surface image a) 800 °C sintered powder b)1250 °C sintered $Ce_{0.85}La_{0.1}Gd_{0.05}O_2$ pellet

Table 1. EDS results powders of 800 oC and $Ce_{0.85}La_{0.1}Gd_{0.05}O_2$ pellet 1250 °C

Element	Seriess .	C norm. [at.%]	C Atom. [wt.%]
Cerium (800 °C)	L-series	85.99	86.35
Lanthanum	L-series	9.47	9.59
Gadolinium	L-series	4.54	4.06
Cerium (1250 °C)	L-series	54.34	81.59
Lanthanum	L-series	6.97	10.47
Gadolinium	L-series	3.85	5.77

on the separate contributions of grain and grain boundaries resistance. Typically, Nyquist plots are observed at three semicirculars: (I) a high frequency semicircular is considered as the grain resistivity, (II) an intermediate frequency semicircular is considered as grain thw boundary resistivity, and (III) a low frequency semicircular is considered to provide information about the contact electrode. In this study, conductivity evaluations were made according to Nyquist plots.

Before conductivity measurements, both surfaces of the pellets were painted with silver paste and then calcined for one hour at 100 °C. The contacts were provided by using binders with platinum wires. The conductivity measurement was performed at a temperature of 400-750 °C. Parstat 2273 software from

Princeton Applied Research was employed for data storage. Measurements were made parametrically in the 100 kHz-100 mHz frequency range. For each data set, a complex plane graph, such as real impedance and imaginary impedance, was prepared. The conductivity values were calculated from the following equation:

$$\sigma = \frac{l}{A.R} \quad (3)$$

Total conductivity: σT
Total resistance: R total
Cross-sectional area: A
Thickness: l

The conductivity of ceria electrolyte depends upon the synthesis method, microstructural factors, sintering temperature, ion radius of dopant type, dope type, rates, etc. [23-28]. The reduction from Ce^{4+} to Ce^{3+} shows the electronic conductivity at high temperature and low oxygen pressure [13]. In addition, the co-dope method is used to overcome the reduction problem. Various combinations are used for different dope types in the literature [27, 29]. In this study, electronic conductivity was suppressed by using co-doped La and Gd. The conductivity measurements are made at low temperatures. As the temperature increases, the resistance decreases and the conductivity increases. The electrical conductivity values of $Ce_{0.85}La_{0.15}Gd_{0.05}O_2$ are shown in Table 2.

Table 2. Conductivity $Ce_{0.85}La_{0.1}Gd_{0.05}O_2$ pellets

Temperature (°C)	Conductivity (S.cm^{-1})
750	0.0022
700	0.0016
675	0.0014
625	0.00054

According to the values in Table 2, when the temperature increases, the resistance decreases and the conductivity increases. Also, the best conductivity and conductivity value were observed at 750 °C and was 0.0022 S.cm^{-1}, respecctively. However, CeO_2 is nonconductive at low temperatures. It becomes conductive and the conductivity value σ depends strongly on the temperature, dope type, and dope ratio. The oxygen-ion conductivity value of pure CeO_2 was $6{,}16\times10^{-5}$ Scm^{-1} at 600 °C [5]. As a result, a higher conductivity in comparison to pure CeO_2 conductivity was obtained with doping type and ratios.

4. Conclusions

This study set out to investigate how to improve the crystal and conductivity values of pure CeO_2. In this respect, several conclusions can be made in light of the obtained results. First, when XRD results were evaluated, a cubic crystal structure was obtained with La and Gd co-doped by CeO_2. Also, the heat and dope type factor positively affected the crystal structure. According to the results of the thermal analysis,

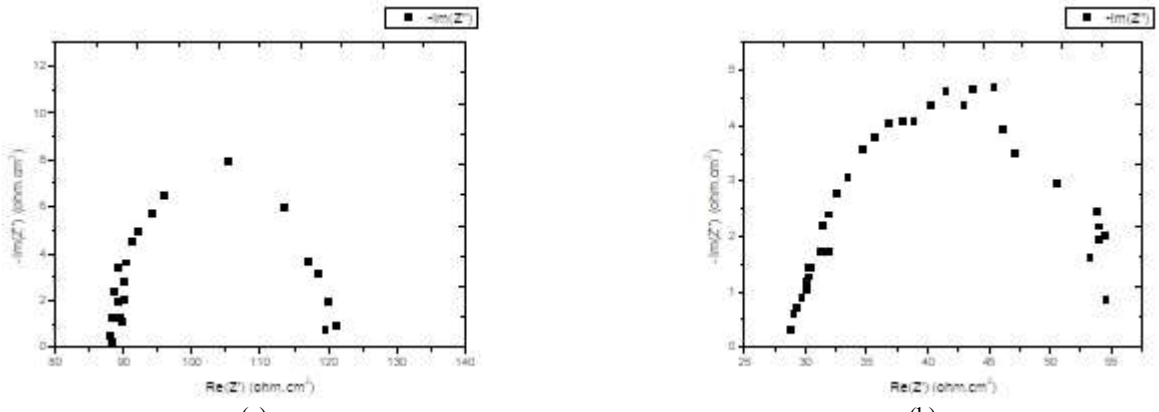

(a) (b)

Fig.5. Nyquist plot of $Ce_{0.85}La_{0.1}Gd_{0.05}O_2$ sample measured in air. a) 625 °C b)750 °C

4. Conclusions

This study set out to investigate how to improve the crystal and conductivity values of pure CeO_2. In this respect, several conclusions can be made in light of the obtained results. First, when XRD results were evaluated, a cubic crystal structure was obtained with La and Gd co-doped by CeO_2. Also, the heat and dope type factor positively affected the crystal structure. According to the results of the thermal analysis, no phase change was observed in the operating temperatures. While the grain size of the sample that was sintered at 800 ^oC powder was 120 nm, the grain size of the sample that was sintered at 1250 ^oC was 2 micron. According to the EDS results, the rates used at the beginning were preserved and the grain was formed at the sintering temperature. Surface porosity almost never occurred. In addition, the conductivity measurement results increased based on temperature, and maximum conductivity was observed at 750 ^oC.

Acknowledgements

In this study, we would like to thank the Kahramanmaraş İstiklal University for providing financial support. We would also like to thank Associate Professor Bora TIMURKUTLUK for his help on the impedance analysis.

References

[1] Ramadhanı F., et al. “Optimization strategies for Solid Oxide Fuel Cell (SOFC) application: A literature survey”, Renewable and Sustainable Energy Reviews, 2017, 76:460.

[2] Yamamoto O., “Solid oxide fuel cells: fundamental aspects and prospects”, Electrochimica Acta, 2000, 45.15-16: 2423.

[3] Kirubakaran A., Jain S., Nema R. K. “A review on fuel cell technologies and power electronic interface”, Renewable and Sustainable Energy Reviews, 2009, 13.9: 2430.

[4] Haile S. M. “Fuel cell materials and components”,Acta Materialia, 2003, 51.19: 5981.

[5] Dudek M., “ Ceramic oxide electrolytes based on CeO_2-preparation, properties and possibility of application to electrochemical devices”, Journal of the European ceramic society, 2008, 28.5: 965.

[6] Hayashi K., et al. “Solid oxide fuel cell stack with high electrical efficiency”, NTT Technical Review, NTT Energy and Environment Systems Laboratories, Japan, 2009.

[7] Williams M. C., Application of power electronics with the US DOE distributed generation programme, Int. J. Energy Technology and Policy, 2007.

[8] Ahmadi R., Pourfatemi SM.,Ghaffari S. “Exergoeconomic optimization of hybrid system of GT, SOFC and MED implementing genetic algorithm”. Desalination, 2017, 411: 76.

[9] Minh N.Q. “Solid oxide fuel cell technology-features and applications”, Solid State Ionics, 2004, 174.1-4: 271.

[10] Kwak SC., Kim B.K., Kim D. I., Cho Y.W “Pulsed Electrodeposition of Thin Cobalt Coating Layer on Ferritic Stainless Steel for SOFC Interconnects” Korean Journal of Metals and Materials, 2017, 55(11): 768.

[11] Morales M., Roa J.J., Tartaj J., Segarra, M. “A review of doped lanthanum gallates as electrolytes for intermediate temperature solid oxides fuel cells: From materials processing to electrical and thermo-mechanical properties”. Journal of the European Ceramic Society, 2016. 36(1): 1.

[12] Gómez S. Y., Hotza D. “Current developments in reversible solid oxide fuel cells”, Renewable and Sustainable Energy Reviews, 2016, 61: 155.

[13] Mahato N., et al. “ Progress in material selection for

solid oxide fuel cell technology: A review" ,Progress in Materials Science, 2015, 72: 141.

[14] Hui S. R., et al. "A brief review of the ionic conductivity enhancement for selected oxide electrolytes", Journal of Power Sources, 2007, 172.2: 493.

[15] Steele B. C. H. " Materials for IT-SOFC stacks: 35 years R&D: the inevitability of gradualness", Solid state ionics, 2000, 134.1-2: 3-2.

[16] Figueiredo F. M. L., Marques F. M. B. "Electrolytes for solid oxide fuel cells", Wiley Interdisciplinary Reviews: Energy and Environment, 2013, 2.1: 52.

[17] Rahaman M. N. Sintering of ceramics. CRC press, 2007.

[18] Devi P. S., Banerjee S. " Search for new oxide-ion conducting materials in the ceria family of oxides" Ionics, 2008, 14.1: 73.

[19] Sun Q., Fu Z., Yang Z. " Effects of rare-earth doping on the ionic conduction of CeO_2 in solid oxide fuel cells" Ceramics International, 2018, 44.4: 3707.

[20] Molenda, J., Świerczek, K., Zając, W. "Functional materials for the IT-SOFC". Journal of Power Sources, 2007, 173.2: 657.

[21] Pikalova E. Y., et al. "Solid electrolytes based on CeO2 for medium-temperature electrochemical devices" Russian Journal of Electrochemistry, 2011, 47.6: 690.

[22] Jin H., et al. "Synthesis and conductivity of cerium oxide nanoparticles" Materials Letters, 2010, 64.11: 1254.

[23] Ou D.R., Mori T., Ye F., Zou J., Drennan J. "Comparison between Y-doped ceria and Ho-doped ceria: Electrical conduction and microstructures. Renewable Energy", 2008, 33(2): 197.

[24] Omar S., et al. "Crystal structure–ionic conductivity relationships in doped ceria systems", Journal of the American Ceramic Society, 2009, 92.11: 2674.

[25] Chou C., Huang C., Yeh T. " Investigation of ionic conductivities of CeO_2-based electrolytes with controlled oxygen vacancies", Ceramics International, 2013, 39: 627.

[26] Bošković S.B., et al. "Doped and Co-doped CeO_2: Preparation and properties", Ceramics international, 2008, 34.8: 2001.

[27] Kobi S., Jaiswal N., Kumar D., Parkash O. "Ionic conductivity of Nd3+ and Y3+ co-doped ceria solid electrolytes for intermediate temperature solid oxide fuel cells". Journal of Alloys and Compounds, 2016, 58: 513.

[28] Rushton M. J. D., Chroneos A. " Impact of uniaxial strain and doping on oxygen diffusion in CeO_2", Scientific reports, 2014, 4: 6068.

[29]Tadokoro S.K., Muccillo E. N.S. "Effect of Y and Dy co-doping on electrical conductivity of ceria ceramics", Journal of the European Ceramic Society, 2007, 27(13-15): 4261.